

In preparation for ApJ, 2006

**Water vapor on supergiants.  
The 12  $\mu\text{m}$  TEXES spectra of  $\mu$  Cephei**

N. Ryde

*Department of Astronomy and Space Physics, Uppsala University, Box 515, SE-75120  
Uppsala, Sweden*

ryde@astro.uu.se

M. J. Richter<sup>1</sup>

*Department of Physics, University of California at Davis, CA 95616*

richter@physics.ucdavis.edu

G. M. Harper

*Center for Astrophysics and Space Astronomy - Astrophysics Research Lab, 593 UCB,  
University of Colorado, Boulder, CO 80309-0593*

gmh@casa.colorado.edu

K. Eriksson

*Department of Astronomy and Space Physics, Uppsala University, Box 515, SE-75120  
Uppsala, Sweden*

kjell.eriksson@astro.uu.se

D. L. Lambert

*Department of Astronomy, University of Texas at Austin, RLM 15.308, USA, TX 78712*

dll@astro.as.utexas.edu

**ABSTRACT**

---

<sup>1</sup>Visiting Astronomer at the Infrared Telescope Facility, which is operated by the University of Hawaii under Cooperative Agreement no. NCC 5-538 with the National Aeronautics and Space Administration, Office of Space Science, Planetary Astronomy Program.

Several recent papers have argued for warm, semi-detached, molecular layers surrounding red giant and supergiant stars, a concept known as a MOLsphere. Spectroscopic and interferometric analyses have often corroborated this general picture. Here, we present high-resolution spectroscopic data of pure rotational lines of water vapor at  $12\ \mu\text{m}$  for the supergiant  $\mu$  Cep. This star has often been used to test the concept of molecular layers around supergiants. Given the prediction of an isothermal, optically thick water-vapor layer in Local Thermodynamic Equilibrium around the star (MOLsphere), we expected the  $12\ \mu\text{m}$  lines to be in emission or at least in absorption but filled in by emission from the molecular layer around the star. Our data, however, show the contrary; we find definite absorption. Thus, our data do not easily fit into the suggested isothermal MOLsphere scenario. The  $12\ \mu\text{m}$  lines, therefore, put new, strong constraints on the MOLsphere concept and on the nature of water seen in signatures across the spectra of early M supergiants. We also find that the absorption is even stronger than that calculated from a standard, spherically symmetric model photosphere without any surrounding layers. A cool model photosphere, representing cool outer layers is, however, able to reproduce the lines, but this model does not account for water vapor emission at  $6\ \mu\text{m}$ . Thus, a unified model for water vapor on  $\mu$  Cep appears to be lacking. It does seem necessary to model the underlying photospheres of these supergiants in their whole complexity. The strong water vapor lines clearly reveal inadequacies of classical model atmospheres.

*Subject headings:* stars: individual ( $\mu$  Cep) – stars: atmospheres– Infrared: stars

## 1. Introduction

Water is a key molecule in the atmospheres of oxygen-rich stars of spectral type late M and cooler. It is one of the most abundant molecules and it is a dominant source of opacity in the infrared. Therefore, it plays an important role both for the photospheric structure and the appearance of infrared spectra. To different degrees it dominates the spectra of brown dwarfs, M-dwarfs and Mira variable stars. Water lines and bands seem to be a common feature of M supergiants and M giants (see for example Tsuji et al. 1997, 1998; Yamamura et al. 1999; Tsuji 2000a,b, 2001a; Verhoelst et al. 2003). While hydrostatic and homogeneous models of stellar atmospheres do not predict water vapor spectral features for stars hotter than late M-type, the existence of water vapor in mid-K to early-M giants was observed from medium-resolution ( $R = \lambda/\Delta\lambda \approx 1600$ ), near-infrared spectra recorded by the *Infrared Space Observatory (ISO)* (Tsuji et al. 1997; Tsuji 2000b, 2001b). These

features are attributed to a static, warm, molecular layer situated within a few stellar radii beyond, and dynamically detached from, the photosphere - an empirical concept known as a MOLsphere (see Tsuji et al. 1997, 1998; Tsuji 2000b; Matsuura et al. 1999) - but distinct from the cool, expanding circumstellar envelope. The water vapor, at temperatures of 1000–2000 K (Tsuji et al. 1997), results in non-photospheric signatures in infrared spectra of M giants. The notion of a molecular layer (MOLsphere) has been used in several cases to explain discrepancies between synthetic spectra and near-infrared observations of late K and M giants and supergiants showing water-vapor features.

Further, mid-infrared spectra with a spectral resolution of  $R \approx 80,000$  revealed water vapor signatures in even warmer stars, such as Arcturus, a K2IIIp giant (Ryde et al. 2002, 2003a). This is the warmest star yet with water vapor features in its disk-averaged spectrum, and it is indeed a surprising discovery. Thus, the presence of water vapor in the spectra of K and M stars is now well established (Tsuji 2003).

In their analysis of the water lines in Arcturus, Ryde et al. (2002, 2003b) argued that the water vapor is photospheric and not circumstellar. The line widths of the water vapor lines match those of the OH lines that are definitely formed in the photosphere (see the discussion in Ryde et al. 2002). No velocity shifts between the water and the OH lines are found. The authors were able to model both the water vapor lines and the OH lines of different excitation by one photospheric model after cooling the temperature structure of the outermost layers to lower than that calculated by a standard model photosphere. The later model requires that the flux is conserved through every layer of the modeled star; at the cooler temperatures, water vapor forms. A further discussion on possible causes for the presence of the water vapor lines is also given. Thus, Ryde et al. (2002) suggest that these lines are formed in the photosphere of the star and that, in order to model these lines, hydrostatic, homogeneous model photospheres assuming *Local Thermodynamic Equilibrium* (LTE) are inadequate. Standard models of the outer photospheres of giants and supergiants omit potentially important physics, such as inhomogeneities that result from large convective motions and the break-down of the assumption of LTE in the calculation of the physical structure of the photosphere.

A challenge to the current understanding of the MOLspheres surrounding M supergiants, are the high-resolution, mid-infrared spectra at  $12 \mu\text{m}$  of the M1-M2 Ia-Iab supergiant Betelgeuse presented by Ryde et al. (2006). They show that neither published MOLsphere models, introduced to account for other observations of Betelgeuse, nor a synthetic spectrum calculated on the basis of a classical model photosphere at the often assumed effective temperature for Betelgeuse, match their spectra. However, with the uncertainties in the outer regions of the photospheric models in mind, they are able to model the lines with a cooler temperature

structure in the line-forming regions. This is the same sort of explanation as they invoked for the existence of water vapor in the spectrum of Arcturus, a star that has no evidence of a MOLsphere. Thus, they argue that it is not necessary to introduce a MOLsphere in order to reasonably explain the 12  $\mu\text{m}$  lines in the spectrum of Betelgeuse. It should be noted that no definitive solution is presented as to the origin of the 12  $\mu\text{m}$  lines that also can explain water-vapor signatures at other wavelengths in the spectrum of Betelgeuse.

To summarize, the location – whether photospheric or circumstellar – and the origin of the water vapor signatures found in a range of K and M giants and supergiants are not clearly and consistently established. However, it is clear that a growing body of spectroscopic data for a range of red giants and supergiants suggests that classical model atmospheres are inadequate (Tsuji 2003). It is unclear whether the water vapor features have a common origin across the range of stars and wavelengths observed. In this present paper, we present observations of the M1-M2 Ia supergiant  $\mu$  Cep, a prototypical MOLsphere case.

## 2. Evidence for water-vapor in $\mu$ Cep

Danielson et al. (1965) suggested that spectral signatures in absorption of vibrational-rotational bands at 1.4  $\mu\text{m}$  (mostly  $\nu_1\nu_2\nu_3 = 101 - 000$  transitions) and 1.9  $\mu\text{m}$  ( $\nu_1\nu_2\nu_3 = 011 - 000$ ) in low-resolution observations of  $\mu$  Cep made with the *Stratoscope II* telescope were due to water vapor. This suggestion of stellar water vapor was, however, overlooked until it was confirmed by Tsuji (2000b), **who in Tsuji (2000a) also** found evidence for water vapor absorption at 2.7  $\mu\text{m}$  ( $\nu_1$  and  $\nu_3$  fundamental vibrational-rotational bands). Furthermore, *ISO* data analysed by Tsuji (2000a) show evidence of water vapor in emission at 6.3  $\mu\text{m}$  ( $\nu_2$  fundamental vibrational-rotational band) and at 40  $\mu\text{m}$  (pure rotational lines). Thus, the 1.4, 1.9, and 2.7  $\mu\text{m}$  features are seen in absorption, whereas the 6.3 and 40  $\mu\text{m}$  features are detected in emission. Tsuji (2000a, 2003) shows, in an intuitive interpretation of the observed data, that this can be achieved and explained elegantly in an optically thick MOLsphere consisting of water vapor. For wavelengths shorter than 5  $\mu\text{m}$  this layer causes absorption while at longer wavelengths the geometrical extension of the water vapor sphere leads to emission, see also Figure 1. This layer is approximately one stellar radius beyond the photosphere, has an excitation temperature of 1500 K and a column density of  $N_{\text{col}}(\text{H}_2\text{O}) = 3 \times 10^{20} \text{ cm}^{-2}$  (Tsuji 2000b, 2003). The temperature of this layer is intermediate between the hot chromosphere and the cold circumstellar matter. The water molecules in the layer are not thought to be of photospheric origin, but rather formed at a distance beyond the photosphere and absent beneath the layer. Perrin et al. (2005) corroborate the idea of molecular layers around  $\mu$  Cep, based on an analysis and modeling of narrow-band spatial

interferometry in the K band.

The first authors to publish observations of stellar  $12\ \mu\text{m}$  lines of water vapor were, to our knowledge, Jennings and Sada (1998) in spectra of Betelgeuse and Antares at a resolution of  $R \approx 8000$ . The  $12\ \mu\text{m}$  pure rotational lines have previously not been observed for the supergiant  $\mu\ \text{Cep}$ , and the interesting question arose as to how these water lines would behave, whether they are in absorption or in emission.

If the MOLsphere scenario with its optically thick water vapor lines is correct, then these lines ought to be in emission, like the  $6.3$  and  $40\ \mu\text{m}$  features, assuming that the lines are optically thick, see Fig. 1. In a photospheric scenario without a major MOLsphere, they would more likely be in absorption. An obvious third possibility is a mixed case of contributions from two components, i.e. a variation of the MOLsphere in which it contributes optically thin emission that weakens the photospheric absorption lines.

In order to investigate the optical depths of water vapor lines from the isothermal MOLsphere, we calculate their optical depths from line data taken from the water vapor line-list of Partridge and Schwenke (1997) and the model parameters in Tsuji (2002b, 2003). At line center,  $\nu_0$ , assuming a thermally broadened line with a characteristic line width of  $\Delta\nu_D = \nu_0/c \times (2kT/m_{\text{H}_2\text{O}})^{1/2}$  we get

$$\tau_{\nu_0}^l \approx 0.02654 \times \frac{N_{\text{col}}}{\sqrt{\pi}\Delta\nu_D} (1 - e^{-h\nu_0/kT}) \frac{g_l f_{lu}}{U(1500\ \text{K})} e^{-\chi/kT}, \quad (1)$$

where  $N_{\text{col}}$  is the column density of water vapor,  $U$  is the partition function of water vapor and has a value of 2713 for a temperature of 1500 K (Partridge and Schwenke 1997), and  $\chi$  is the excitation energy of the level. In Figure 2 we plot this optical depth for water vapor from  $1$  to  $77\ \mu\text{m}$ . From the figure we can immediately see that there are optically thick water vapor lines in all wavelength bands, in agreement with the conclusion of Tsuji (2000b, 2003). In particular, many  $12\ \mu\text{m}$  lines are optically very thick. As an illustration, from Eq. 1 and using line data presented in Table 2, we see that  $\tau_{\nu_0}^l \approx 200$  for the water line at  $818\ \text{cm}^{-1}$ .

### 3. Observations and data reduction

Our observations of  $\mu\ \text{Cep}$  were made with TEXES, the Texas Echelon-cross-Echelle Spectrograph (Lacy et al. 2002), at the *IRTF*. The observations were made at the start of the night of Dec 2, 2000 (UT) to confirm the telescope focus and registration of the telescope acquisition camera with the TEXES entrance slit for subsequent science targets.

We observed in the TEXES high spectral resolution mode. The spectral resolution, as determined by Gaussian fits to telluric atmospheric lines, has a FWHM equivalent to  $R = 65000$  or  $4.6 \text{ km s}^{-1}$ . The slit width was  $1.5''$  and the length  $8''$ . The cross-dispersed spectrum included 9 separate orders covering the spectral range from  $813.59 \text{ cm}^{-1}$  to  $819.48 \text{ cm}^{-1}$ . We used telluric lines to determine that our wavelength scale is accurate to  $0.4 \pm 0.6 \text{ km s}^{-1}$ . At this setting, the individual spectral orders are larger than the  $256^2$  pixel detector, resulting in slight gaps in the final, extracted spectrum.

Two data files were saved to disk. Each file consists of 16 nod-pairs where we nodded  $10''$  North-South to take the target completely off the slit. We integrated for 2 seconds on either side of the nod. On later TEXES observation runs, we found this pattern to be quite inefficient and now integrate 6-8 seconds before nodding the telescope. Total integration time for  $\mu \text{ Cep}$  is 64 seconds.

Before each data file, we observed a calibration sequence consisting of an ambient temperature blackbody, a low emissivity surface, and blank sky. Subtracting sky from the blackbody provides a telluric absorption spectrum suitable for establishing the wavelength scale. Furthermore, the black-sky difference frame gives an approximate correction for telluric interference; if the sky, telescope, and instrument optics were all at a single uniform temperature, then dividing by the black-sky difference would, in theory, perfectly correct for telluric absorption.

We reduced the data according to standard procedures described in Lacy et al. (2002). The spectra were extracted using the spatial profile along the slit for each file. Data from the two files were then combined with weighting according to the effective integration time (the square of the signal-to-noise ratio).

In each order we fitted a  $5^{th}$  order polynomial to normalize the continuum. Spectral regions with stellar and telluric features were given low weight in the fit. We expect any systematic uncertainties in the polynomial fits to reduce the equivalent widths determined by roughly 10% (Ryde et al. 2006).

#### 4. The observed spectra of $\mu \text{ Cep}$

In Figures 3 and 4 we show our recorded spectrum of  $\mu \text{ Cep}$ , shifted to the laboratory frame. The orders of the spectrometer are shown by the vertical lines. **Four** water line features are clearly detected, namely those at  $815.90 \text{ cm}^{-1}$  (**a pure rotational line within the first excited vibrational state,  $\nu_2$** ),  $816.15 - 816.19 \text{ cm}^{-1}$  (also pure rotational lines within the first excited vibrational state,  $\nu_2$ ),  $816.69 \text{ cm}^{-1}$  (**a rotational line within the**

ground state), and the two lines at  $818.42 \text{ cm}^{-1}$  (**also rotational lines within the ground state**). Two OH lines of a quartet are also identified. Three of these lie within the wavelength range observed. One of these ( $814.7 \mu\text{m}$ ) and the water lines at  $815.3$ ,  $816.45$ , and  $817.15 \mu\text{m}$  have not been identified, most probably because of problems with sky subtraction and noise, and the difficulties in the continuum subtraction. In Tables 1 and 2 we give the observational data measured from these spectra. Although we have measured only very few lines, the lines are found to be shifted by the same amount, namely  $\langle \Delta v_{\text{OH}} \rangle = 23.9 \pm 1.4 \text{ km s}^{-1}$  and  $\langle \Delta v_{\text{water}} \rangle = 21.3 \pm 1.1 \text{ km s}^{-1}$  in the frame of the observer.

Table 1: Observational data of pure rotational, OH lines.

$\tilde{\nu}_{\text{lab}}$	$E''_{\text{exc}}$	$\log gf$	$v' - v''$	Lower level	$\tilde{\nu}_{\text{lab}} - \tilde{\nu}_{\text{obs}}$	Obs. Equivalent Width <sup>a</sup>	FWHM <sup>a</sup>
[cm <sup>-1</sup> ]	[eV]				[10 <sup>-3</sup> cm <sup>-1</sup> ]	[10 <sup>-3</sup> cm <sup>-1</sup> ]	[km s <sup>-1</sup> ]
814.7280	1.297	-1.57	0-0	R <sub>1e</sub> 24.5	-	-	-
815.4032	1.302	-1.58	0-0	R <sub>2e</sub> 23.5	63	2.5	22
815.9535	1.300	-1.57	0-0	R <sub>1f</sub> 24.5	68	4.5:	26:

<sup>a</sup>A colon (:) marks measured values with large uncertainties.

Table 2: Observational data and the line list of the water-vapor lines.

$\tilde{\nu}_{\text{lab}}$	$E''_{\text{exc}}$	$\log gf$	$J'K'_aK'_cJ''K''_aK''_c$	$v_1v_2v_3$	$\tilde{\nu}_{\text{lab}} - \tilde{\nu}_{\text{obs}}$	Equivalent width	FWHM
[cm <sup>-1</sup> ]	[eV]				[10 <sup>-3</sup> cm <sup>-1</sup> ]	[10 <sup>-3</sup> cm <sup>-1</sup> ]	[km s <sup>-1</sup> ]
816.157	1.467	-1.109					
816.151	1.467	-1.586					
816.15525	1.150	-1.301	22 13 10 21 12 9	(010)	57	1.7	17
816.179	2.721	-1.241					
816.179	2.721	-0.764					
816.18551	1.150	-1.778	22 13 9 21 12 10	(010)			
816.68703	1.014	-1.35	24 12 13 23 11 12	(000)	62	1.5	15
818.4238 <sup>c</sup>	1.029	-1.66	22 16 6 21 15 7	(000)			
818.4247 <sup>c</sup>	1.029	-1.19	22 16 7 21 15 6	(000)	56	1.8	21

<sup>c</sup>Assignments from Tsuji (2000b).



## 5. The modelling of the spectra of $\mu$ Cep

We have modeled the photospheric spectrum at 12  $\mu\text{m}$  of  $\mu$  Cep and a spectrum generated by a MOLsphere surrounding the star.  $\mu$  Cep is not identical to Betelgeuse but is a supergiant resembling Betelgeuse (Tsuji 2000b; Verhoelst et al. 2006). Therefore, we have used our photospheric model of Betelgeuse, as presented in Ryde et al. (2006) as a typical supergiant model to which our data will be compared. We assume that this model is a reasonable representation of the photosphere of  $\mu$  Cep.

The model photosphere we used was calculated with the MARCS code (Gustafsson et al. 2003). These hydrostatic, spherical model photospheres are computed assuming LTE, chemical equilibrium, homogeneity, and the conservation of the total flux (radiative plus convective; the convective flux being computed using the mixing length recipe). The radiation field used in the model generation is calculated with absorption from atoms and molecules by opacity sampling at approximately 95 000 wavelength points over the wavelength range 1300  $\text{\AA}$ –20  $\mu\text{m}$ . The models are calculated with 56 depth points from a Rosseland optical depth of  $\log \tau_{\text{Ross}} = 2.0$  out to  $\log \tau_{\text{Ross}} = -5.0$ , which in our case corresponds to an optical depth evaluated at 500 nm of  $\log \tau_{500} = -4.1$ . The physical height above the  $\log \tau_{\text{Ross}} = 0$  layer of this outermost point is  $2.8 \times 10^{12}$  cm or 6% of the stellar radius. Extending the model out to  $\tau_{\text{Ross}} = -5.6$  affects the water-vapor lines only marginally.

Our stellar parameters, used as input for the model photosphere calculation are  $T_{\text{eff}} = 3600$  K,  $\log g = 0.0$ , solar metallicity (except for the C, N, and O abundances),  $M = 15 M_{\odot}$  (implying  $R = 650 R_{\odot}$ ),  $\xi_{\text{micro}} = 4 \text{ km s}^{-1}$  (microturbulence) and  $\xi_{\text{macro}} = 7 \text{ km s}^{-1}$  (macroturbulence). As a comparison Levesque et al. (2005) deduce an effective temperature of 3700 K for  $\mu$  Cep and find a  $\log g = -0.5$ . The C, N, and O abundances are  $A_{\text{C}} = 8.29^1$ ,  $A_{\text{N}} = 8.37$ , and  $A_{\text{O}} = 8.52$ . The decreased carbon abundance and the increased nitrogen abundance compared to solar values are consistent with signatures of the expected first dredge-up which massive stars like Betelgeuse and  $\mu$  Cep experience. The signatures are those of CN-cycled material which affects the surface abundances since the convective envelope of the star during the first dredge-up reaches down to nuclear-processed regions of the interior (Lambert et al. 1984). The most abundant molecules in the deep atmosphere are molecular hydrogen, CO, OH, CN, and CH. Above the layer defined by  $\log \tau_{\text{Rosseland}} = -1$ , water starts to form and its abundance becomes greater than that of CN and CH.

The isothermal, spherical MOLsphere, assumed to be in LTE, is characterized by an inner and an outer radius, a single temperature, and a column density of water vapor.

---

<sup>1</sup>The abundance by number  $N_{\text{C}}$  is given through the following definition:  $A_{\text{C}} \equiv \log N_{\text{C}} - \log N_{\text{H}} + 12$

The parameters of the MOLsphere of  $\mu$  Cep that we have used are those discussed by Tsuji (2000a), namely  $T = 1500$  K,  $R_{\text{in}} = 2 R_{\star}$ ,  $R_{\text{out}} = 4 R_{\star}$ , and  $N_{\text{col}} = 3 \times 10^{20} \text{ cm}^{-1}$ . The density in the levitated MOLsphere is assumed to be in hydrostatic equilibrium in the gravity field of the star (Tsuji 2000a), thus in some unknown way being supported at the inner radius. The density structure decreases almost exponentially outwards from the inner boundary with a scale height which is very much smaller than the shell thickness. We have further assumed a microturbulence velocity in the MOLsphere of  $4 \text{ km s}^{-1}$  and introduced a macroturbulence of  $v_{\text{D}} = 7 \text{ km s}^{-1}$ , with which we convolve the synthetic spectrum. The background flux shining onto the MOLsphere is given by the synthetic spectrum based on our photosphere ( $T_{\text{eff}} = 3600$  K).

The synthetic spectra of the photosphere and MOLsphere were calculated for points on the spectrum separated by  $\Delta\tilde{\nu} \sim 1 \text{ km s}^{-1}$  (corresponding to a resolution of  $\tilde{\nu}/\Delta\tilde{\nu} \sim 300\,000$ ) even though the final resolution is lower. In the radiative transfer calculation of the MOLsphere component we use 22 rays on the stellar disk, and 53 shells around the star. Our models (both the model photosphere and MOLsphere, and the synthetic spectra based on them) are calculated in spherical geometry. The photosphere has a modeled extension ( $\Delta R_{\text{atm}}/R_{\star}$ ) of approximately 5%. Calculations in spherical symmetry will generally tend to decrease the strengths of strong lines in the mid- and far-infrared. In extreme cases even photospheric emission may appear. The reason for this is that an extended photosphere will occupy a larger solid angle at line wavelengths where the total opacity is large. This will result in a larger flux at line centers and therefore weaker lines than those resulting from calculations in plane-parallel geometry. A MOLsphere will naturally cause emission in optically thick lines due to its large geometrical size.

The line list in our calculation of the photospheric synthetic spectra is described in Ryde et al. (2002) and is based on the work by Polyansky et al. (1996, 1997). The wavelengths of the lines in the list are sufficiently accurate for the resolution of the observations. However, only the strongest lines are included. For the temperatures in our model photosphere only the strongest lines do indeed emerge, thus justifying the use of the line list. The data of the water lines in the calculation of the MOLsphere are, however, taken from the line-list of Partridge and Schwenke (1997), which is more complete than the one used for the photospheric spectrum, but the wavelengths are not as accurate as those used for the photosphere. For the cold temperature of the MOLsphere a completeness of the line list is more important than the accuracy of the wavelengths of the lines. The continuous opacities in the MOLsphere from  $\text{H}^{-}$  free-free (ff) and  $\text{H}$  ff are included in our calculation.

Following Tsuji (1978, 2003) we assume an optically thin dust envelope with  $\tau_{10\mu\text{m}} = 0.1$ , that contributes only continuous emission veiling the photospheric line spectrum. Assuming

a distance of approximately  $390 \pm 140$  pc (Perrin et al. 2005), the slit corresponds to  $(9 \pm 3) \times 10^{15}$  cm, which corresponds to approximately 200 stellar radii on the sky. Contrary to the case of Betelgeuse, which lies approximately three times closer to us, we here assume that the entire dust envelope is within the slit and that all dust emission is recorded (cf. the discussion by Ryde et al. 2006). From the *ISO* low-resolution 2-40  $\mu\text{m}$  data and the continuum from a classical model photosphere presented in Tsuji (2003), we have estimated the dust contribution at 12  $\mu\text{m}$  to be  $f_{\text{dust}}^{\text{thin}} = (\text{Flux}_{\text{star+dust}} - \text{Flux}_{\text{star}})/(\text{Flux}_{\text{star+dust}}) = 77\%$  which is the value we use. Note, however, that this value is uncertain and will affect the lines strengths directly.

## 6. Discussion

In addition to the OH lines in absorption, we have observed and identified **four** clear *absorption* features due to rotational transitions of water vapor at 12  $\mu\text{m}$  from the supergiant  $\mu$  Cep. On the basis of the MOLsphere **scenario we expected the water lines to be in emission**. The interpretation of these lines is not straight-forward.

The observed absorption lines at 12  $\mu\text{m}$  leads us to two separate complications associated with the formation of the water lines at 12  $\mu\text{m}$ . **First, the model, proposed in this Section, that fits the spectra implies cooler regions in the outer photosphere where the lines are formed compared to what is expected from a classical model photosphere. The line velocities, widths and depths are evidence for a photospheric origin of the water absorption, but the model photosphere needed for the outer regions does not fulfill the assumptions of a classical model photosphere. The proposed reasons for the break-down of the classical assumptions are an inhomogeneous photosphere, or non-LTE conditions. Second, why water-vapor lines show up in emission at 6.3 and 40  $\mu\text{m}$  but not at 12  $\mu\text{m}$  is unexplained, but this fact should contain a clue to the atmospheric environment of  $\mu$  Cep and further modelling and discussion of these features is needed. It can neither be explained by a simple photosphere with a cooler outer structure, since that predicts all water lines across the spectrum to be in absorption, nor can it be explained by an optically thick, isothermal MOLsphere. Therefore, it would be of great interest to try to understand the 12  $\mu\text{m}$  spectra combined with all other spectroscopic water vapor data and interferometric data, and try to explain them all in terms of a consistent, unified picture, since  $\mu$  Cep is a prototypical MOLsphere case (Tsuji 2000a). A consistent scenario which can account for the water-vapor features and the nature of water in supergiants is lacking.**

**Some sort of non-classical atmosphere is clearly needed, but the challenge to explain all features in one model still prevails.**

### 6.1. A cooler outer photosphere?

In Figures 3 and 4 we have also plotted our model spectra based on a photosphere of an effective temperature of 3600 K, the assumed temperature of  $\mu$  Cep. The spectrum includes the contribution of the optically thin dust emission. While we see from the figures that the OH quartet, unfortunately represented by only one clean line, is quite well modeled with our combined photospheric and optically-thin dust model, the water vapor lines show stronger absorption than one would expect from a classical model photosphere. Changing the effective temperature of the model photosphere by  $\pm 100$  K affects the equivalent widths of the water-vapor lines by approximately  $\pm 50\%$ , and an increase of  $\log g$  by 0.3 dex increases the lines' strengths by approximately 40%, far from what is needed to model the observed absorption lines.

The water vapor lines and OH lines both depend on the partial pressure of oxygen in the same way. However, the lines of these two molecules react differently to a change in temperature. In order to fit the water lines, a photospheric model of an effective temperature of 3250 K is needed. A synthetic spectrum based on such a cold model is plotted in the figures as well. The fit is very good for both the OH and the various water vapor lines. It should be noted, however, that there is not a very large range in excitation energies of the water lines (1.014 – 1.150 eV). Ideally, a test of a model structure would include lines of different excitations. The cooler model of 3250 K was also used for the similar case of Betelgeuse in order to model  $12\ \mu\text{m}$  spectra (Ryde et al. 2006). These authors discuss the details of this model, such as the differences in C, N, and O abundances between the models.

An effective temperature of 3250 K is out of the range of possible temperatures for  $\mu$  Cep. As mentioned in Section 1, a way of interpreting the cold temperature structure that fits the  $12\ \mu\text{m}$  lines, is that classical models fail to describe relevant physical features such as inhomogeneities, structures not in LTE, etc in supergiants. The colder structure could be representing cold convective elements in an inhomogeneous photosphere. Alternatively, the cooler model could be simulating a colder outer photosphere in the regions where the water-vapor lines are formed. It would, therefore, be interesting to investigate the influence of inhomogeneities due to convection on the water-vapor lines and the detailed effects on the spectra of a change of the outermost atmospheric structure, which is known to be uncertain. We will address these questions in a forthcoming paper.

The turbulent line-widths of the  $12\ \mu\text{m}$  lines and the OH lines (which are resolved at  $R = 65000$  or  $4.6\ \text{km s}^{-1}$ ) are of the same order in both  $\mu\text{Cep}$  and Betelgeuse. Apart from the different amounts of circumstellar dust, these two supergiants seem to behave in the same way concerning the  $12\ \mu\text{m}$  lines. As was discussed in Ryde et al. (2006) the line widths in Betelgeuse indicated a photospheric origin. Furthermore, there is no significant velocity shift between the OH and the water vapor lines. This finding is similar to what we found for other stars we have analysed; Arcturus (K1.5III, Ryde et al. 2002) and Betelgeuse (M1-2 Ia-Iab, Ryde et al. 2006). Thus, based on their line widths and velocities, the observed  $12\ \mu\text{m}$  lines in  $\mu\text{Cep}$  look like photospheric absorption lines. As a note, if the  $12\ \mu\text{m}$  lines were formed in a MOLsphere, this water layer would need to have large turbulent velocities and no expansion velocity.

To summarize, a photosphere with a non-classical outer structure is able to describe the mid-infrared spectra, both the OH and water vapor lines. Furthermore, the lack of velocity shifts and the line widths are nicely explained. However, this explanation does not explain other infrared and interferometric data (Perrin et al. 2005). Thus, the simple photosphere with a cooler outer structure can not explain all observed features since that model predicts all water lines across the spectrum to be in absorption.

## 6.2. A modified MOLsphere?

As we have noted, earlier investigations of  $\mu\text{Cep}$  have shown that vibrational-rotational water-vapor bands in the near-infrared are formed in absorption while the vibrational-rotational  $\nu_2$  band at  $6.3\ \mu\text{m}$  and the rotational lines at  $40\ \mu\text{m}$  are observed in emission (Tsuji 2000b). This behavior is explained with an optically thick, isothermal MOLsphere consisting of water vapor (Tsuji 2000b). To directly fit into this MOLsphere concept with optically thick lines, the rotational lines at  $12\ \mu\text{m}$  are expected to be in emission too. We now see the opposite. Figure 5 shows the result of a calculation of the MOLsphere for  $\mu\text{Cep}$ , which clearly does not explain the observed spectrum.

How can we modify the MOLsphere model so that it better predicts the  $12\ \mu\text{m}$  lines? We have not solved this problem, but we discuss a few suggestions here.

- From Figure 1 we see directly that, assuming that the lines are optically thick, it would be possible to construct a MOLsphere that would give absorption lines at  $12\ \mu\text{m}$  by changing the size of the modeled molecular layer. This effect is also explained nicely by Ohnaka (2004). This change would, however, at the same time lead to the  $6\ \mu\text{m}$  lines also being in absorption, which is not observed (Tsuji 2000a).

Despite the assumed similarities between the supergiants  $\mu$  Cep and Betelgeuse, the nature of the observed water vapor is somewhat different, which is discussed by Tsuji (2000a). Contrary to the case of  $\mu$  Cep, the *ISO* spectrum of Betelgeuse shows the  $\nu_2$  water band at  $6.3 \mu\text{m}$  in absorption (Tsuji 2000a). However, the rotational lines at  $40 \mu\text{m}$  in *ISO* spectra of Betelgeuse could also be interpreted as emission, similar to what is seen in the spectra of  $\mu$  Cep (Tsuji 2000a). The mid-infrared spectra of Betelgeuse show rotational lines at  $12 \mu\text{m}$  in absorption (Jennings and Sada 1998; Ryde et al. 2006), similar to our  $\mu$  Cep observations. Thus, the two stars show some differences in the nature of the water assumed to be surrounding them. Tsuji (2000a) suggests that the inner boundary of the surrounding assumed water-vapor envelope is closer to the star in the case of Betelgeuse, which could explain that the  $6.3 \mu\text{m}$  data are in absorption and not the  $40 \mu\text{m}$  features. However, the MOLsphere suggested by Tsuji (2000a) does not fit the high-resolution spectra at  $12 \mu\text{m}$  either (Ryde et al. 2006).

- The MOLsphere model is based on the assumption that the relative strengths of the different water lines and bands are given by the excitation temperature of  $T_{\text{ex}} = 1500 \text{ K}$  through a Boltzmann distribution affecting their opacities. This may, however, be questionable. For example, Hinkle and Lambert (1975) show, for diatomic molecules, that even in the outer regions of a photosphere of a supergiant like  $\alpha$  Ori, collisions are not dominant over radiative processes for vibration-rotational transitions. In the case of water-vapor, the relevant rotational transitions have very strong transition probabilities, even stronger than the probabilities of relevant vibration-rotation lines. This means that radiation may well be the dominant transition process, leading to scattering by water-vapor lines. If scattering in the optically-thick lines is allowed for, absorption may be the result. All line photons will be scattered and eventually a fraction of these will be absorbed by the medium, implying that fewer photons escape. However, this process has to differentiate between the long-wavelength rotational lines which are seen in emission and the rotational lines at  $12 \mu\text{m}$  which are seen in absorption. Also, light from the surrounding dust, which shines strongly at  $12 \mu\text{m}$ , will be scattered by the  $12 \mu\text{m}$  lines and has to be incorporated. Thus, a full non-LTE analysis of a water vapor layer in the radiation field of the star and the dust would have to be performed. This possibility should be tested in future MOLsphere models.

If light resonantly scattered in molecular lines is important, special care has to be taken when comparing spectra from various instruments with different beam sizes. For example, while the slit dimensions of the SWS spectrometer onboard *ISO* is  $14'' \times 20''$  at  $6 \mu\text{m}$ , the slit of the TEXES spectrometer is  $8'' \times 1.5''$ . More scattered light may therefore be recorded by *ISO* than by TEXES. This could be an **explanation** to why

*ISO* measured emission at 6  $\mu\text{m}$  and TEXES absorption at 12  $\mu\text{m}$ .

- Another way of modifying the isothermal MOLsphere interpretation is to allow for temperature gradients. This could be tuned to give absorption lines, but should be physically reasonable. Again, the emission at 6 and 40  $\mu\text{m}$  **also** has to be explained.

Thus, it would be interesting to investigate different implementations and modifications of a MOLsphere lying beyond a calculated photosphere of a generic M supergiant (representing the cases of  $\mu$  Cep and Betelgeuse) or a semiempirical model photosphere, and to test these against all available data.

## 7. Conclusions

We have pointed to the accumulating amount of independent evidence for the existence of water vapor in K and M giants and supergiants. Explaining existing water lines, bands, and interferometric data of supergiants appears, however, to be a challenge. In order to understand the origin of the unexpected water vapor, it seems that we have to go beyond classical modelling, be it a MOLsphere scenario, models relaxing the assumptions of homogeneity and LTE, or both. No consistent unified model, which can without modifications account for all available data, exists today.

$\mu$  Cep is a test bench for the MOLsphere concept, introduced to explain a range of unexplained observational features, both interferometric and spectroscopic, albeit at low spectral resolution. The new high-resolution, spectroscopic water-vapor 12  $\mu\text{m}$  data presented here do not fit into the current MOLsphere model that can explain other infrared and interferometric data of  $\mu$  Cep. In a non-modified, optically-thick version, the 12  $\mu\text{m}$  lines were expected to be in emission, but the opposite is found. Furthermore, a pure photospheric model predicts much too weak absorption lines for the effective temperature expected for the supergiant. We show that a photosphere with a cooler temperature structure in the line-forming regions of the 12  $\mu\text{m}$  lines is able to fit the spectra, possibly providing a clue to their origin. This indicates that a cooler structure due to, for instance, convective motions, can explain the recorded water-vapour and OH lines. A problem is that this model does not account for the emission at 6  $\mu\text{m}$ .

Thus, a consistent picture is still lacking. It is time for more elaborate modelling and to acquire more high-quality data, especially high-resolution infrared spectra of, for example, **the 1.4, 1.9, 2.7, 6.3, and 40  $\mu\text{m}$**  wavelength regions. Furthermore, measurements with the Atacama Large Millimeter Array (ALMA) at frequencies of 100-700 GHz will be able to

resolve scales at which the MOLsphere should show up. Interferometric observations of the angular diameter as a function of frequency will reveal the nature of the MOLspheres, their existence and their density structure. Note, however, that for  $\mu$ Cep the spatial scales of ALMA are not as well matched as for Betelgeuse, a star also assumed to have a MOLsphere. Future studies will have to show whether a modified MOLsphere scenario in addition to more sophisticated photospheric models are able to simulate all spectroscopic and interferometric data available. Our new data need to be incorporated in any model or scenario of the atmospheres of  $\mu$  Cep in particular and of supergiants in general.

We have once again shown that pure rotational lines of water vapor in the mid-infrared, observed with high-resolution spectrographs, are interesting diagnostics of the atmospheres of (super-)giant stars. The usefulness of the lines is connected with their relatively large transition probabilities and their location in an uncrowded part of the spectrum.

We would like to thank Bengt Gustafsson and John H. Lacy for fruitful suggestions and enlightening discussions. We acknowledge the support we received from John H. Lacy, Daniel T. Jaffe, and Qingfeng Zhu of the TEXES team during the observations of  $\mu$  Cep. We are grateful for the help of the IRTF staff. This work was supported in part by the Swedish Research Councils (VR and STINT), the Robert A. Welch Foundation of Houston, Texas, NSF grant AST-0307497 and NASA grant NNG04GG92G. Observations with TEXES were supported by NSF grant AST-0205518.

## REFERENCES

- Danielson, R. E., Woolf, N. J., and Gaustad, J. E., 1965, *ApJ* 141, 116
- Gustafsson, B., Edvardsson, B., Eriksson, K., Jørgensen, U. G., Mizuno-Wiedner, M., and Plez, B., 2003, in *IAU Symposium 210: 'Modelling of Stellar Atmospheres*, Eds. N. Piskunov, W. W. Weiss, and D. F. Gray, pp CD–A4
- Hinkle, K. H. and Lambert, D. L., 1975, *MNRAS* 170, 447
- Jennings, D. E. and Sada, P. V., 1998, *Science* 279, 844
- Lacy, J. H., Richter, M. J., Greathouse, T. K., Jaffe, D. T., and Zhu, Q., 2002, *PASP* 114, 153
- Lambert, D. L., Brown, J. A., Hinkle, K. H., and Johnson, H. R., 1984, *ApJ* 284, 223



- Levesque, E. M., Massey, P., Olsen, K. A. G., Plez, B., Josselin, E., Maeder, A., and Meynet, G., 2005, *ApJ* 628, 973
- Matsuura, M., Yamamura, I., Murakami, H., Freund, M. M., and Tanaka, M., 1999, *A&A* 348, 579
- Ohnaka, K., 2004, *A&A* 421, 1149
- Partridge, H. and Schwenke, D., 1997, *J. Chem. Phys.* 106, 4618
- Perrin, G., Ridgway, S. T., Verhoelst, T., Schuller, P. A., Coudé Du Foresto, V., Traub, W. A., Millan-Gabet, R., and Lacasse, M. G., 2005, *A&A* 436, 317
- Polyansky, O. L., Busler, J. R., Guo, B., Zhang, K., and Bernath, P. F., 1996, *J. Mol. Spectrosc.* 176, 305
- Polyansky, O. L., Tennyson, J., and Bernath, P. F., 1997, *J. Mol. Spectrosc.* 186, 213
- Ryde, N., Harper, G. M., Richter, M. J., Greathouse, T. K., and Lacy, J. H., 2006, *ApJ* 637, 1040
- Ryde, N., Lacy, J. H., Richter, M. J., Lambert, D. L., and Greathouse, T. K., 2003a, in *ASSL Vol. 283: Mass-Losing Pulsating Stars and their Circumstellar Matter*, p. 227
- Ryde, N., Lambert, D. L., Richter, M. J., and Lacy, J. H., 2002, *ApJ* 580, 447
- Ryde, N., Lambert, D. L., Richter, M. J., Lacy, J. H., and Greathouse, T. K., 2003b, in *ASP Conf. Ser. 293: 3D Stellar Evolution*, p. 214
- Tsuji, T., 1978, *A&A* 68, L23
- Tsuji, T., 2000a, *ApJ Lett.* 540, L99
- Tsuji, T., 2000b, *ApJ* 538, 801
- Tsuji, T., 2001a, in *IAU Symposium 205: 'Galaxies and their Constituents at the Highest Angular Resolutions*, Ed. R. T. Schilizzi, p. 316
- Tsuji, T., 2001b, *A&A* 376, L1
- Tsuji, T., 2003, in *ESA SP-511: Exploiting the ISO Data Archive. Infrared Astronomy in the Internet Age*, p. 93
- Tsuji, T., Ohnaka, K., Aoki, W., and Yamamura, I., 1997, *A&A* 320, L1

- Tsuji, T., Ohnaka, K., Aoki, W., and Yamamura, I., 1998, *Ap&SS* 255, 293
- Verhoelst, T., Decin, L., Van Malderen, R., Hony, S., Cami, J., et al., 2006, *A&A* 447, 311
- Verhoelst, T., Decin, L., Vandenbussche, B., Van Malderen, R., and Waelkens, C., 2003, in *IAU Symposium 210: 'Modelling of Stellar Atmospheres*, Eds. N. Piskunov, W. W. Weiss, and D. F. Gray, pp CD–E14
- Yamamura, I., de Jong, T., and Cami, J., 1999, *A&A* 348, L55

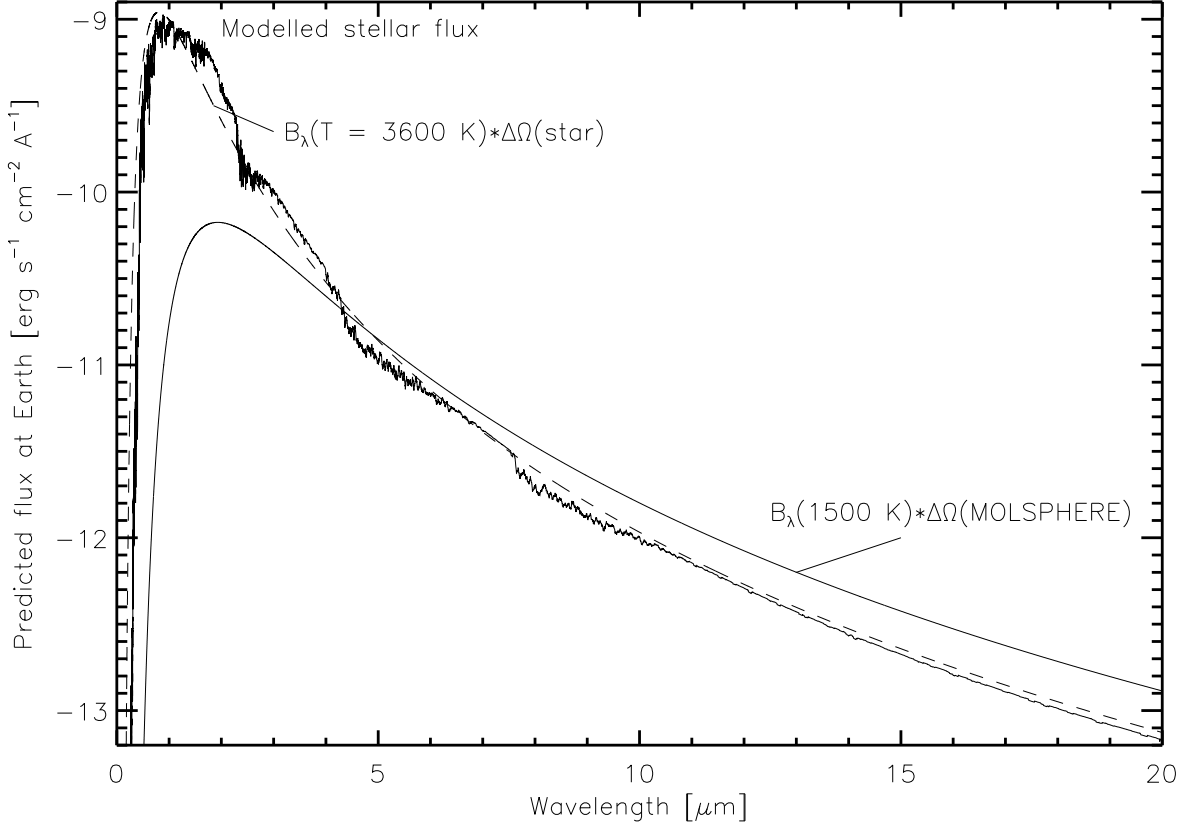


Fig. 1.— Model Spectral Energy Distribution of  $\mu$  Cep is plotted together with a flux from the corresponding Planck function of the stellar effective temperature and assuming a radius of the star of  $650 R_{\odot}$  and a distance to it of 390 pc (Perrin et al. 2005). Furthermore, the flux from the isothermal MOLsphere is plotted as calculated from a Planck function of 1500 K and assuming a radius of the MOLsphere of approximately two stellar radii. For optically thick lines this gives the flux in the lines. From the figure it is evident that optically thick lines are expected to be in absorption for wavelengths shorter than approximately  $5 \mu\text{m}$  and in emission for longer wavelengths, in accordance with Tsuji (2000a, 2003).

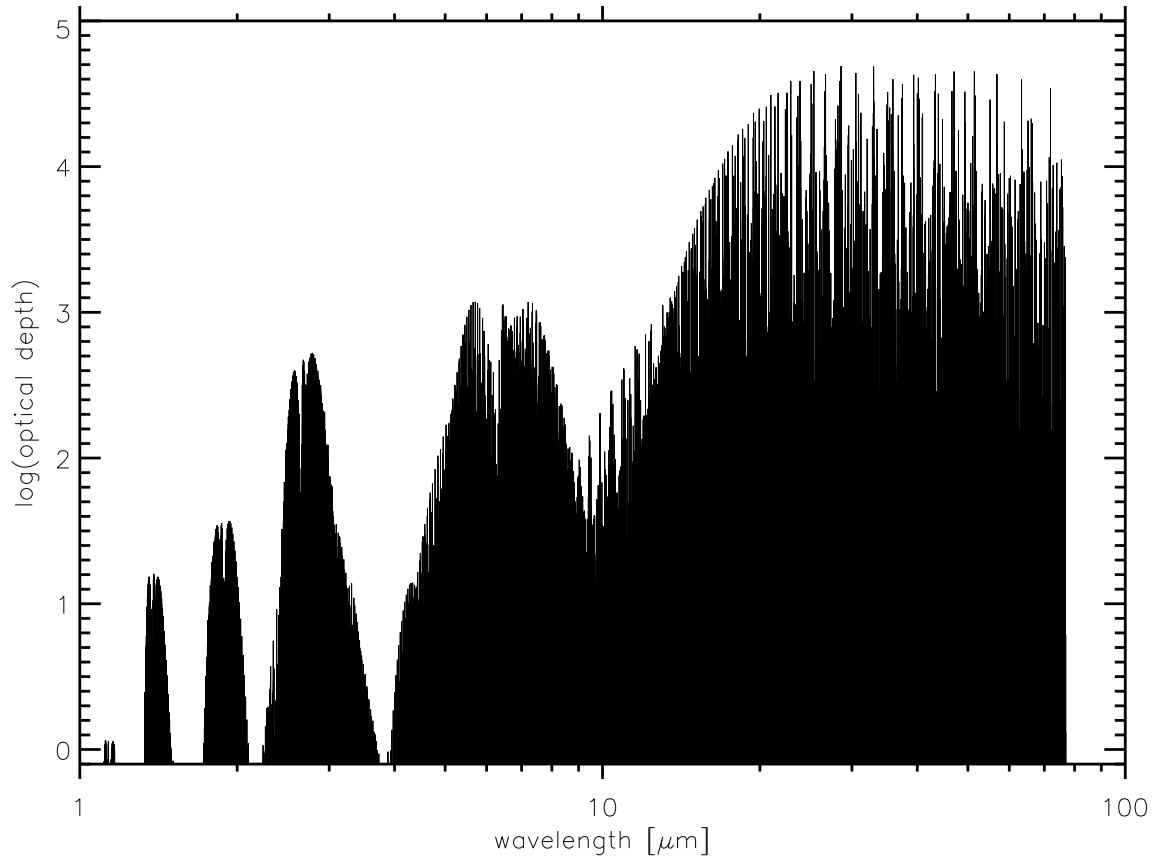


Fig. 2.— The logarithmic optical depth of water-vapor lines from 1 to 77  $\mu\text{m}$  in the isothermal MOLsphere scenario. The temperature is assumed to be 1500 K and the column density  $3 \times 10^{20} \text{ cm}^{-2}$  (Tsuji 2000b, 2003).

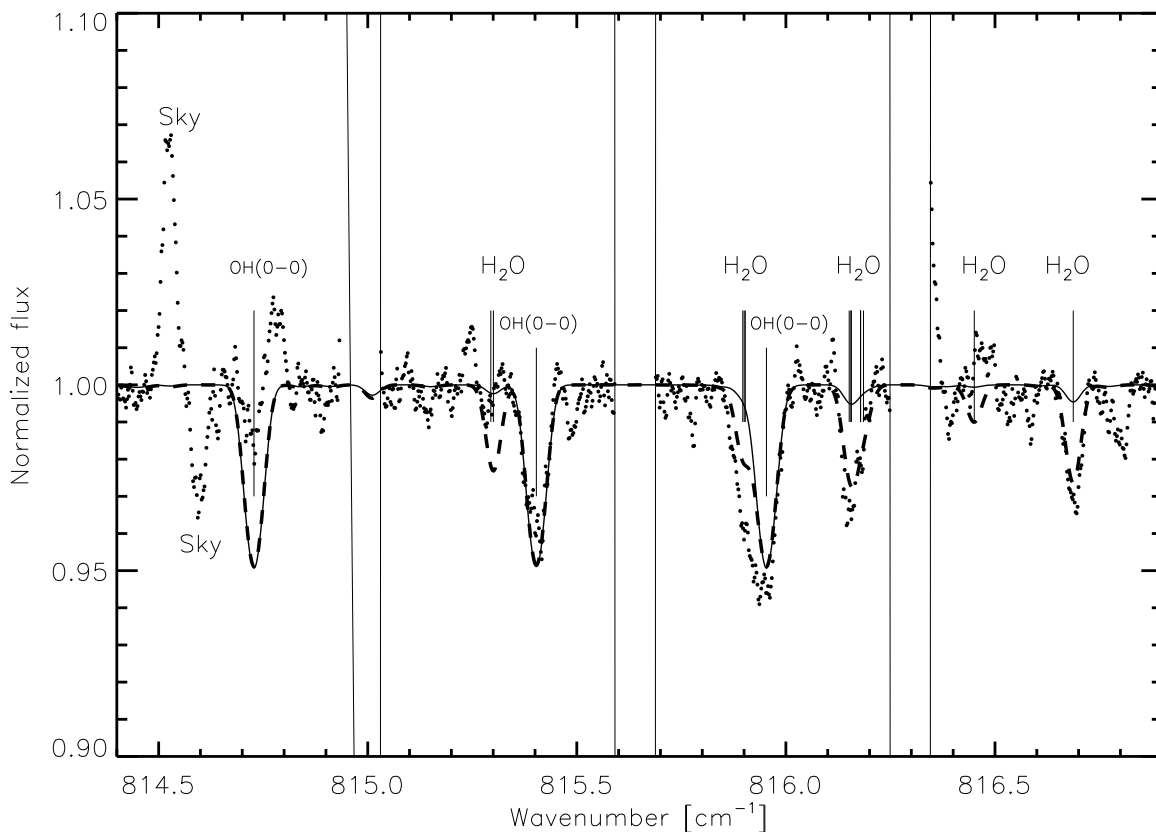


Fig. 3.— Recorded normalized flux spectrum of  $\mu$  Cep is shown with dots. The wavelength range spans  $12.23 - 12.28 \mu\text{m}$ . Our synthetic spectrum, based on a classical model photosphere with an effective temperature of 3600 K, combined with an expected optically thin dust continuum, is shown by the full line together with the observed spectrum. A synthetic spectrum based on a temperature of 3250 K is shown by a dashed line. The orders, which are approximately  $0.5 \text{ cm}^{-1}$  wide are marked with the vertical lines. The most important lines are identified and marked.

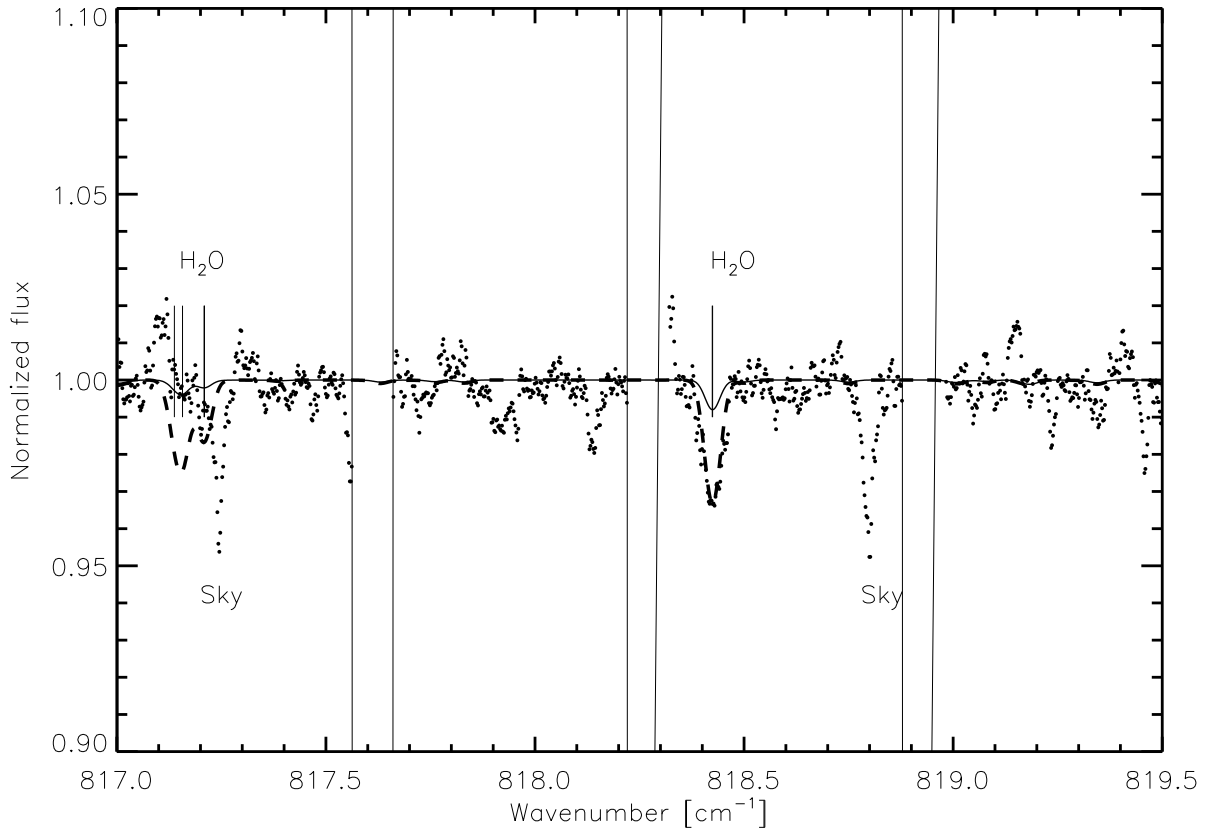


Fig. 4.— The continuation of the spectrum, see legend of Figure 3.

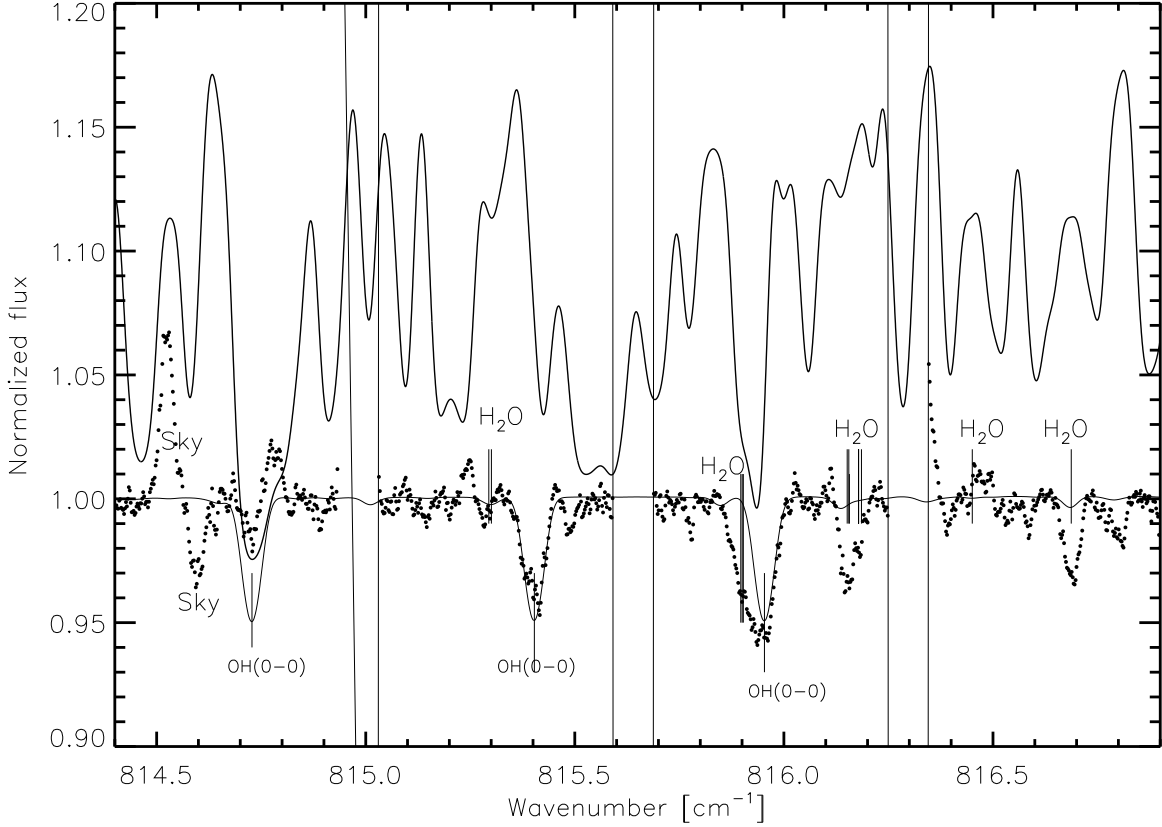


Fig. 5.— The normalized, observed spectrum of  $\mu$  Cep from 12.24 -12.28  $\mu\text{m}$  is shown by dots. The full line with a continuum at 1.0 is a photospheric spectrum calculated with the Partridge and Schwenke (1997) line list. The MOLsphere results shown as the emission spectrum by the full line above the observations are calculated with  $T = 1500$  K,  $R_{\text{in}} = 2 R_{\star}$ ,  $R_{\text{out}} = 4 R_{\star}$ , and  $N_{\text{col}} = 3 \times 10^{20} \text{ cm}^{-1}$ . This spectrum is plotted on the same ordinate scale as the other two spectra. We see that the large, optically thick MOLsphere results in huge emission features which are not seen in the observations. The continuum in the MOLsphere is due to free-free H and  $\text{H}^{-}$  emission, but this continuous opacity is very small. This leads to an optically very thin continuum in the MOLsphere which means that it is transparent in the continuum. One of the photospheric absorption lines of OH is not fully filled in by water vapor emission. The other two are. Note, that this MOLsphere realization does not include OH lines in the calculation.